Fluorescence-lifetime-based tomography for turbid media

Anand T. N. Kumar

Athinoula A. Martinos Center for Biomedical Imaging, Massachusetts General Hospital, Harvard Medical School, Charlestown, Massachusetts 02129

Jesse Skoch and Brian J. Bacskai

Alzheimer's Disease Research Unit, Department of Neurology, and Athinoula A. Martinos Center for Biomedical Imaging, Massachusetts General Hospital, Harvard Medical School, Charlestown, Massachusetts 02129

David A. Boas and Andrew K. Dunn

Athinoula A. Martinos Center for Biomedical Imaging, Massachusetts General Hospital, Harvard Medical School, Charlestown, Massachusetts 02129

We derive a novel algorithm to recover the *in vivo* distributions of fluorophores based on an asymptotic lifetime analysis of time-domain fluorescence measurements with turbid tissue. We experimentally demonstrate the advantage offered by this method in localizing fluorophores with distinct lifetimes. This algorithm has wide applicability for diagnostic fluorescence imaging in the presence of several-centimeter-thick biological tissue, since fluorescence lifetime is a sensitive indicator of local tissue environment and interactions at the molecular level. © 2005 Optical Society of America

   OCIS codes: 170.3880, 170.3650.

The recent development of disease-targeted fluorescent markers has prompted concurrent advances in noninvasive optical molecular imaging techniques, promising an alternative to positron emission tomography and magnetic resonance imaging for diagnostic imaging of diseases and for drug development.[1] Fluorescence optical tomographic technologies utilize continuous wave (CW) excitations,[2] and the frequency domain,[3,4] (FD) or pulsed excitation in the time domain[5–7] (TD). CW systems are low cost and offer high resolution and sensitivity but are incapable of measuring lifetimes. FD techniques can be used to recover fluorescence yield and the lifetime as distributions within the biological medium of interest from surface measurements of intensity and phase. Tomographic measurements are required in the FD, since the detected phase on the medium surface is invariably a mixture of the phase due to the fluorescence lifetime and that due to tissue photon migration. TD techniques offer the potential advantage of direct measurement of lifetime by means of multiple exponential fits to fluorescence decays, an aspect well exploited for nonscattering thin tissue samples by microscopy techniques such as fluorescence lifetime imaging (FLIM).[8] In the presence of several-centimeter-thick biological tissue, the asymptotic decay of TD fluorescence will be affected by the diffuse propagation of light within the tissue. In this Letter we address TD fluorescence measurements with diffuse media and show that the intrinsic fluorophore lifetime can be directly obtained from asymptotic TD data for a wide range of tissue optical properties of biomedical interest. More important, we demonstrate a rigorous algorithm for the separate 3-D yield reconstruction of multiple fluorophores with distinct *in vivo* lifetimes by using decay amplitudes extracted from TD data. Lifetime-sensitive fluorescent dyes are

widely employed in FLIM techniques to provide high-resolution 2-D spatial lifetime maps of thin tissue sections, thereby revealing biochemical processes in tissues and elementary molecular interactions.[9] The method presented here, on the other hand, offers a natural way to extend the application of lifetime sensitive fluorescent probes to 3-D *in vivo* imaging in several-centimeter-thick turbid tissue.

   Let the fluorophores within the biological medium of interest be described by yield distributions $\eta_n(\mathbf{r})$ with corresponding lifetimes $\tau_n = 1/\Gamma_n$. We start by writing the TD fluorescence signal as a Fourier transform of the FD counterpart, written in its adjoint form.[3] The detected fluorescence intensity at position $\mathbf{r}_d$ and time t due to excitation by a point source at $\mathbf{r}_s$ and at time $t=0$ is then given in the Born approximation, which considers a single fluorophore absorption and emission event, by (omitting scaling coefficients for simplicity):

$$U_F(\mathbf{r}_d,\mathbf{r}_s,t) = \sum_n \int_{-\infty}^{\infty} d\omega e^{-i\omega t}$$

$$\times \int_V d^3 r \left[\tilde{G}_m(\mathbf{r}_d,\mathbf{r},\omega) \frac{i\Gamma_n \eta_n(\mathbf{r})}{\omega + i\Gamma_n} \tilde{\Phi}_x(\mathbf{r},\mathbf{r}_s,\omega) \right], \quad (1)$$

where $\tilde{\Phi}_x(\mathbf{r},\mathbf{r}_s,\omega)$ and $\tilde{G}_m(\mathbf{r}_d,\mathbf{r},\omega)$ are the FD Green's function and fluence for the excitation light from a point source to the fluorophore and emission from the fluorophore to the detector, respectively, and the volume integration is over the extent of the medium. To get more physical insight, we examine the analytic nature (in the complex variable sense) of the integrand in Eq. (1) using the FD Green's functions for an infinite homogeneous medium, which are of the form $\exp(ik_{x,m}r)/4\pi D_{x,m}r$ with $k_{x,m}^2 = (-v\mu_{a_{x,m}}$

$+i\omega)/D_{x,m}$, where the subscripts x, m denote excitation and emission wavelengths. The quantities $\mu_{a_{x,m}}$, $D_{x,m}(=v/3\mu'_{s_{x,m}})$, and $\mu'_{s_{x,m}}$ denote, respectively, the absorption, diffusion, and reduced scattering coefficients, and v is the velocity of light in the medium. It is evident that the homogeneous Green's function and its spatial derivatives are bivalued owing to the square root in k, implying branch points in the lower half-plane at $\omega=-iv\mu_{a_x},-iv\mu_{a_m}$. In addition, the integrand in Eq. (1) possesses simple pole singularities distributed along the negative imaginary axis at $\omega_n=-i\Gamma_n$. On applying Cauchy's theorem,[10] it is possible to show that U_F separates into two parts, the first corresponding to fluorescence decay terms (arising from the residues at the simple poles) and the other corresponding to a diffuse photon density wave (arising from integration around the branch points):

$$U_F(\mathbf{r}_d,\mathbf{r}_s,t) = \sum_n a_{F_n}(\mathbf{r}_d,\mathbf{r}_s)\exp(-\Gamma_n t)$$
$$+ a_D(\mathbf{r}_d,\mathbf{r}_s,t)\exp(-v\mu_a t), \qquad (2)$$

where we have set $\mu_a=\mu_{a_x}=\mu_{a_m}$, without any loss of generality of the results to follow. The amplitude a_{F_n} of the decay of the nth fluorophore is readily obtained as the residue at the simple pole[10] at $-i\Gamma_n$ and is in the form of a linear inverse problem for the yield distribution $\eta_n(\mathbf{r})$ of the nth fluorophore:

$$a_{F_n}(\mathbf{r}_d,\mathbf{r}_s) = \int_V d^3 r\, W_n(\mathbf{r}_s,\mathbf{r}_d,\mathbf{r})\,\eta_n(\mathbf{r}), \qquad (3)$$

where the weight matrix for the inversion is given by

$$W_n = \Gamma_n \widetilde{G}_m(\mathbf{r}_d,\mathbf{r},\omega=-i\Gamma_n)\widetilde{\Phi}_x(\mathbf{r},\mathbf{r}_s,\omega=-i\Gamma_n). \quad (4)$$

The coefficient a_D [second term on the right-hand side of Eq. (2)] is calculated as the contribution from the branch points and is not presented in detail here. Although the above results were derived assuming a homogeneous infinite medium, their general validity may be argued as follows. Since a general solution for the inhomogeneous diffusion equation in a bounded volume may be written in terms of the homogeneous Green's function and its normal derivatives at the boundary,[11] it is plausible to assert that the complex plane structure of the integrand in Eq. (1) is reproduced for bounded, inhomogeneous media. This implies that Eq. (4), which results from the contribution of the simple poles, can be generalized to arbitrary media by simply replacing the Green's functions with solutions of the heterogeneous diffusion equation for finite boundary models. We performed Monte Carlo simulations (not shown for brevity) with finite boundaries to confirm the applicability of Eq. (3) to finite heterogeneous media. We further demonstrate the algorithm experimentally for a homogeneous slab medium below.

The inverse problem as expressed in Eqs. (3) and (4) and the subsequent generalization to arbitrary media constitute the central result of this Letter and enable separate reconstructions of multiple fluorophores from an asymptotic analysis of TD fluorescence data. In order for these equations to be applicable to biomedical imaging, it is first essential to determine the conditions for which the first term of Eq. (2) is dominant, i.e., when the decay times of the measured signal are governed purely by the fluorescence lifetimes. It has been noted[12] that the decay of time-resolved signals is affected by diffuse propagation effects for strongly scattering and weakly absorbing tissue and for short fluorophore lifetimes. The key quantity of interest is the asymptotic diffusive decay time, which for semi-infinite media[13] reduces to the absorption time scale $\tau_{abs}[=(v\mu_a)^{-1}]$. The presence of finite boundaries will likely alter this asymptotic behavior. We study this quantitatively in Fig. 1, where the decay times of simulated diffusive TD signals are shown as a contour plot for a wide range of optical properties, assuming a slab medium, and for thicknesses (Z) 2 and 10 cm. It is seen from Fig. 1 that the asymptotic decay time is longer for smaller absorption and larger reduced scattering. The region of optical properties for which the fluorescence decay with a given lifetime is asymptotically dominant can be read from Fig. 1 as the darker shaded regions to the right of the contour with the corresponding decay time. Overall, the results of Fig. 1 show that for optical properties relevant to biomedical imaging ($\mu'_s < 30$ cm^{-1}, $\mu_a > 0.01$ cm^{-1}) the decay time of the TD diffusive response is shorter than typically encountered fluorophore lifetimes ($\tau > 0.5$ ns), suggesting that fluorescence lifetimes may be extracted asymptotically from TD measurements. Note that for heterogeneous media the smallest absorption present in the medium should be considered when Fig. 1 is used to determine the decay time.

Assuming that the lifetime is longer than the diffusive time scales (see Fig. 1), the first term of Eq. (2) dominates the asymptotic behavior of TD fluorescence signals and can be used to extract fluorophore locations based on a lifetime analysis. Since $\widetilde{G}_{x,m}(\mathbf{r}_d,\mathbf{r},\omega=-i\Gamma)$ are solutions to the CW diffusion equation (Helmholtz wave equation) with a reduced
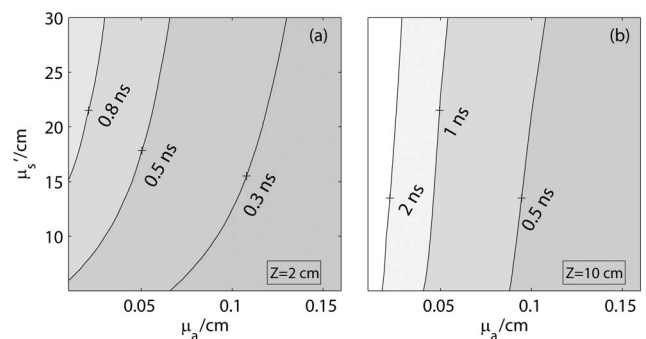

Fig. 1.   Simulated contours of constant asymptotic decay time of TD diffuse signals as a function of absorption and reduced scattering. The simulations assumed a perturbation at the center of a homogeneous slab, with a single-source–detector pair in the transmission geometry. Slab thickness (a) 2 cm, (b) 10 cm. The darker shaded region to the right of each contour gives the optical properties for which a fluorescence decay with lifetime corresponding to the contour lifetime can be recovered asymptotically from TD measurements.

absorption of $\mu_{a_{x,m}}(\mathbf{r}) - \Gamma_n/v$, the weight matrix W_n for the inverse problem in Eq. (3) is identical to that of a CW problem. Thus, when multiple lifetimes are present, a tomographic TD measurement separates asymptotically into equivalent CW measurements, each with only one lifetime component present. This factorization vastly simplifies the computational complexity of the fluorescence TD problem for long times, which normally requires a double convolution.

In Fig. 2 we experimentally demonstrate the application of lifetime-based tomography. We used a near-infrared dye from LI-COR Biosciences, with absorption and emission maxima at ≈ 770 and 790 nm. Two polyethylene tubes were placed with a 4.5 mm vertical separation in a Petri dish filled with Intralipid +ink solution, with the dye mixed in aqueous and glycerol solvents. The presence of glycerol increases the excited state lifetime due to an increased viscosity. The data were collected in a transmission geometry by using a TD molecular imaging system consisting of a Spectra-Physics Ti:sapphire laser source (100 fs pulse width, 80 MHz repetition rate, 770 nm excitation), and a gated intensified CCD camera from LaVision (500 ps gate width, 560 V gain, 100 ms integration time). The light output from the laser was attenuated to a few milliwatts and launched into a 200 μm fiber by using a fiber collimation package. The other end of the fiber was mounted on a computer controlled motorized translation stage placed below the dish containing the tubes. The light exiting the fiber was focused onto the surface of the dish by using another collimation package and served as the source. The full temporal fluorescence signal was collected at 830 nm by using a 10 nm width bandpass filter for a line of 41 sources and 41 detectors placed 1 mm apart across the tube (detectors were assigned on the camera image). The lifetime components were determined directly from a subset of the data with high signal-to-noise ratio to be 0.5 and 0.8 ns, and the amplitude of each component was estimated for all the source–detector pairs by using a linear fit with fixed lifetimes. Figure 2 shows the x–z slice of 3-D reconstructions by using the amplitudes in Eq. (3), compared with the standard FD reconstruction. The vertical separation of the tubes was estimated from the peaks of the depth dependent fluorescence yield for the two lifetime components as 4.25 mm. The standard FD approach, however, fails to resolve the axially located inclusions, with the reconstruction located between the true depths of the tubes [Fig. 2(b)].

In summary, we have presented a fluorescence tomography algorithm based on an asymptotic lifetime analysis of TD fluorescence signals. In this algorithm, the *in vivo* fluorescence lifetimes are obtained directly from TD measurements, and the 3-D fluorophore distribution that contributes to each lifetime component is obtained as a separate reconstruction. The use of lifetime as a parameter thus allows for a significant improvement in the localization ability of fluorescence tomography. While TD techniques have been exploited well in FLIM microscopy with thin tissues, we suggest the method proposed here as a to-
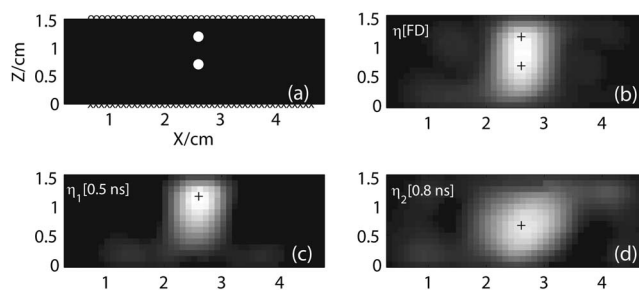

Fig. 2.   Demonstration of lifetime-based tomography with experimental data. (a) Measurement geometry, with two tubes (0.5 mm inner diameter) immersed at depths 1.2 and 0.7 cm in an Intralipid+ink solution ($\mu_a = 0.1$ cm^{-1}, $\mu_s' = 10$ cm^{-1}) in a phantom, and filled with fluorophores of lifetimes 0.5 and 0.8 ns, respectively. (b) Reconstruction of fluorescence yield by using the FD diffusion model. (c) (d), Reconstruction using the amplitudes of the 0.5 and the 0.8 ns decay components in Eq. (3). The + signs are the true fluorophore locations for reference.

mographic extension of FLIM to turbid media. This approach could serve as a potentially highly relevant tool for optical imaging in noninvasive disease diagnostics and for drug discovery and development, given the increasing development of lifetime-sensing fluorescent molecular probes. We note that the method proposed here is applicable to more general source–detector geometries than the transmission case considered here. In future work, we will explore the application of lifetime-based tomography to *in vivo* small-animal imaging.

References

1. V. Ntziachristos, J. Ripoll, L. V. Wang, and R. Weissleder, Nat. Biotechnol. **23**, 314 (2005).
2. V. Ntziachristos and R Wessleder, Opt. Lett. **26**, 893 (2001).
3. M. A. Oleary, D. A. Boas, X. D. Li, B. Chance, and A. G. Yodh, Opt. Lett. **21**, 158 (1996).
4. A. Godavarty, E. M. Sevick-Muraca, and M. J. Eppstein, Med. Phys. **32**, 992 (2005).
5. G. M. Turner, G Zacharakis, A. Sourbet, J. Ripoll, and V. Ntziachristos, Opt. Lett. **30**, 409 (2003).
6. K. Chen, L. T. Perelman, Q. G. Zhang, R. R. Dasari, and M. S. Feld, J. Biomed. Opt. **5**, 144 (2000).
7. M. E. Zevallos, S. K. Gayen, B. B. Das, M. Alrubaiee, and R. R. Alfano, IEEE J. Sel. Top. Quantum Electron. **5**, 916 (1999).
8. P. I. H. Bastiaens and A. Squire, Trends Cell Biol. **9**, 48 (1999).
9. P. R. Selvin, Nat. Struct. Biol. **7**, 730 (2000).
10. J. Matthews and R. L. Walker, *Mathematical Methods of Physics*, 2nd ed. (Addison-Wesley, 1970).
11. G. Barton, *Elements of Green's Functions and Propagation* (Oxford U. Press, 1989).
12. M. S. Patterson and B. W. Pogue, Appl. Opt., **33**, 1963 (1994).
13. M. S. Patterson, B. Chance, and B. C. Wilson, Appl. Opt. **28**, 2331 (1989).